

Original citation:

LHCb Collaboration (Including: Back, J. J., Blake, Thomas, Craik, Daniel, Dossett, D., Gershon, T. J., Kreps, Michal, Latham, Thomas, Pilar, T., Poluektov, Anton, Reid, Matthew M., Silva Coutinho, R., Wallace, Charlotte and Whitehead, M. (Mark)). (2014) Study of the kinematic dependences of $\Lambda b 0$ production in pp collisions and a measurement of the $\Lambda b 0 \rightarrow \Lambda c + \pi -$ branching fraction. Journal of High Energy Physics, Volume 2014 (Number 8). Article number 143.

Permanent WRAP url:

<http://wrap.warwick.ac.uk/63619>

Copyright and reuse:

The Warwick Research Archive Portal (WRAP) makes this work of researchers of the University of Warwick available open access under the following conditions.

This article is made available under the Creative Commons Attribution 4.0 International license (CC BY 4.0) and may be reused according to the conditions of the license. For more details see: <http://creativecommons.org/licenses/by/4.0/>

A note on versions:

The version presented in WRAP is the published version, or, version of record, and may be cited as it appears here.

For more information, please contact the WRAP Team at: publications@warwick.ac.uk

warwick**publications**wrap

highlight your research

<http://wrap.warwick.ac.uk>

Study of the kinematic dependences of Λ_b^0 production in pp collisions and a measurement of the $\Lambda_b^0 \rightarrow \Lambda_c^+ \pi^-$ branching fraction



The LHCb collaboration

E-mail: l.carson@ed.ac.uk

ABSTRACT: The kinematic dependences of the relative production rates, $f_{\Lambda_b^0}/f_d$, of Λ_b^0 baryons and B^0 mesons are measured using $\Lambda_b^0 \rightarrow \Lambda_c^+ \pi^-$ and $\bar{B}^0 \rightarrow D^+ \pi^-$ decays. The measurements use proton-proton collision data, corresponding to an integrated luminosity of 1 fb^{-1} at a centre-of-mass energy of 7 TeV, recorded in the forward region with the LHCb experiment. The relative production rates are observed to depend on the transverse momentum, p_T , and pseudorapidity, η , of the beauty hadron, in the studied kinematic region $1.5 < p_T < 40 \text{ GeV}/c$ and $2 < \eta < 5$. Using a previous LHCb measurement of $f_{\Lambda_b^0}/f_d$ in semileptonic decays, the branching fraction $\mathcal{B}(\Lambda_b^0 \rightarrow \Lambda_c^+ \pi^-) = (4.30 \pm 0.03 \text{ }^{+0.12}_{-0.11} \pm 0.26 \pm 0.21) \times 10^{-3}$ is obtained, where the first uncertainty is statistical, the second is systematic, the third is from the previous LHCb measurement of $f_{\Lambda_b^0}/f_d$ and the fourth is due to the $\bar{B}^0 \rightarrow D^+ \pi^-$ branching fraction. This is the most precise measurement of a Λ_b^0 branching fraction to date.

KEYWORDS: Hadron-Hadron Scattering, B physics, Heavy quark production, Branching fraction, Particle and resonance production

ARXIV EPRINT: [1405.6842](https://arxiv.org/abs/1405.6842)

Contents

1	Introduction	1
2	Detector and simulation	3
3	Event selection	3
4	Event yields	4
5	Results	6
6	Systematic uncertainties	9
7	Conclusions	11
	The LHCb collaboration	14

1 Introduction

Measurements of beauty hadron production in high-energy proton-proton (pp) collisions provide valuable information on fragmentation and hadronisation within the framework of quantum chromodynamics [1]. The study of beauty baryon decays also provides an additional channel for investigating CP violation [2]. While significant progress has been made in the understanding of the production and decay properties of beauty mesons, knowledge of beauty baryons is limited.

The relative production rates of beauty hadrons are described by the fragmentation fractions f_u, f_d, f_s, f_c and $f_{\Lambda_b^0}$, which describe the probability that a b quark fragments into a B_q meson (where $q = u, d, s, c$) or a Λ_b^0 baryon, respectively, and depend on the kinematic properties of the b quark. Strange b baryons are less abundantly produced [3] and are neglected here. Measurements of ground state b hadrons produced at the pp interaction point also include decay products of excited b hadrons. In the case of B mesons, such excited states include B^* and B^{**} mesons, while Λ_b^0 baryons can be produced via decays of Λ_b^{*0} or $\Sigma_b^{(*)}$ baryons.

Knowledge of the relative production rate of Λ_b^0 baryons is necessary to measure absolute Λ_b^0 branching fractions. The measurement of the branching fraction of the $\Lambda_b^0 \rightarrow \Lambda_c^+ \pi^-$ decay reported in this paper improves the determination of any Λ_b^0 branching fraction measured relative to the $\Lambda_b^0 \rightarrow \Lambda_c^+ \pi^-$ decay. The inclusion of charge conjugate processes is implied throughout this paper. The average branching fraction and production ratios are measured.

Previous measurements of $f_{\Lambda_b^0}/f_d$ have been made in e^+e^- collisions at LEP [4], $p\bar{p}$ collisions at CDF [5, 6] and pp collisions at LHCb [7]. The value of $f_{\Lambda_b^0}/f_d$ measured at LEP differs significantly from the values measured at the hadron colliders, indicating a strong dependence of $f_{\Lambda_b^0}/f_d$ on the kinematic properties of the b quark.

The LHCb analysis [7] was based on semileptonic $\Lambda_b^0 \rightarrow \Lambda_c^+ \mu^- \bar{\nu} X$ and $\bar{B} \rightarrow D \mu^- \bar{\nu} X$ decays, where the B meson is charged or neutral, and X represents possible additional decay products of the b hadron that are not included in the candidate reconstruction. Near equality of the inclusive semileptonic decay width of all b hadrons was assumed. The analysis measured $f_{\Lambda_b^0}/(f_u + f_d)$, which can be converted into $f_{\Lambda_b^0}/f_d$ under the assumption of isospin symmetry, i.e. $f_u = f_d$. A clear dependence of $f_{\Lambda_b^0}/f_d$ on the transverse momentum p_T of the $\Lambda_c^+ \mu^-$ and $D \mu^-$ pairs was observed. A CMS analysis [8] using $\Lambda_b^0 \rightarrow J/\Psi \Lambda$ decays also found that the cross-section for Λ_b^0 baryons fell faster with p_T than the b -meson cross-sections.

The present paper uses a data sample, corresponding to an integrated luminosity of 1 fb^{-1} of pp collision data at a centre-of-mass energy of 7 TeV, collected with the LHCb detector. This is a substantially increased data sample compared to that in ref. [7]. The analysis aims to clarify the extent and characteristics of the p_T dependence of $f_{\Lambda_b^0}/f_d$. Moreover, the dependence of $f_{\Lambda_b^0}/f_d$ on the pseudorapidity η , defined in terms of the polar angle θ with respect to the beam direction as $-\ln(\tan \theta/2)$, is studied for the first time. The analysis covers the fiducial region $1.5 < p_T < 40 \text{ GeV}/c$ and $2 < \eta < 5$.

The hadronic decays $\Lambda_b^0 \rightarrow \Lambda_c^+ \pi^-$ and $\bar{B}^0 \rightarrow D^+ \pi^-$ are used, with the charm hadrons reconstructed using the decay modes $\Lambda_c^+ \rightarrow p K^- \pi^+$ and $D^+ \rightarrow K^- \pi^+ \pi^+$, respectively. The data sample and the selection of $\bar{B}^0 \rightarrow D^+ \pi^-$ decays are identical to those used in ref. [9]. Although a precise measurement of the absolute value of $f_{\Lambda_b^0}/f_d$ is not possible with these decays, since the $\Lambda_b^0 \rightarrow \Lambda_c^+ \pi^-$ branching fraction is poorly known [10], they can be used to measure the dependence of $f_{\Lambda_b^0}/f_d$ on the b -hadron kinematic properties to high precision. This is achieved by measuring the efficiency-corrected yield ratio \mathcal{R} in bins of p_T or η of the beauty hadron

$$\mathcal{R}(x) \equiv \frac{N_{\Lambda_b^0 \rightarrow \Lambda_c^+ \pi^-}(x)}{N_{\bar{B}^0 \rightarrow D^+ \pi^-}(x)} \times \frac{\epsilon_{\bar{B}^0 \rightarrow D^+ \pi^-}(x)}{\epsilon_{\Lambda_b^0 \rightarrow \Lambda_c^+ \pi^-}(x)}, \tag{1.1}$$

where N is the event yield, ϵ is the total reconstruction and selection efficiency, and x denotes p_T or η . The quantity \mathcal{R} is related to $f_{\Lambda_b^0}/f_d$ through

$$\begin{aligned} \frac{f_{\Lambda_b^0}}{f_d}(x) &= \frac{\mathcal{B}(\bar{B}^0 \rightarrow D^+ \pi^-)}{\mathcal{B}(\Lambda_b^0 \rightarrow \Lambda_c^+ \pi^-)} \times \frac{\mathcal{B}(D^+ \rightarrow K^- \pi^+ \pi^+)}{\mathcal{B}(\Lambda_c^+ \rightarrow p K^- \pi^+)} \times \mathcal{R}(x) \\ &\equiv \mathcal{S} \times \mathcal{R}(x), \end{aligned} \tag{1.2}$$

where \mathcal{S} is a constant scale factor.

Since the value of $f_{\Lambda_b^0}/f_d$ in a given bin of p_T or η is independent of the decay mode of the b hadron, the values of $f_{\Lambda_b^0}/f_d(p_T)$ from the semileptonic analysis [7] can be compared to the measurement of $\mathcal{R}(p_T)$, which allows for the extraction of the value of \mathcal{S} . The branching fraction $\mathcal{B}(\Lambda_b^0 \rightarrow \Lambda_c^+ \pi^-)$ can then be readily obtained using eq. (1.2). Notably, the dependence on $\mathcal{B}(\Lambda_c^+ \rightarrow p K^- \pi^+)$ cancels when extracting $\mathcal{B}(\Lambda_b^0 \rightarrow \Lambda_c^+ \pi^-)$ in this way, because this branching fraction also enters in the semileptonic measurement of $f_{\Lambda_b^0}/f_d$. Furthermore, the branching fractions $\mathcal{B}(\bar{B}^0 \rightarrow D^+ \pi^-)$ [10] and $\mathcal{B}(D^+ \rightarrow K^- \pi^+ \pi^+)$ [11] are well known, leading to a precise determination of $\mathcal{B}(\Lambda_b^0 \rightarrow \Lambda_c^+ \pi^-)$.

The dependence of the semileptonic $f_{\Lambda_b^0}/f_d$ measurement on $\mathcal{B}(\Lambda_b^0 \rightarrow \Lambda_c^+ \mu^- \bar{\nu} X)$, and the assumption of near equality of the inclusive semileptonic decay width of all b hadrons, implies that the measurement of $\mathcal{B}(\Lambda_b^0 \rightarrow \Lambda_c^+ \pi^-)$ from the current paper cannot be used to normalise existing measurements of $\mathcal{B}(\Lambda_b^0 \rightarrow \Lambda_c^+ \mu^- \bar{\nu} X)$ [10].

2 Detector and simulation

The LHCb detector [12] is a single-arm forward spectrometer covering the pseudorapidity range $2 < \eta < 5$, designed for the study of particles containing b or c quarks. The detector includes a high-precision tracking system consisting of a silicon-strip vertex detector surrounding the pp interaction region, a large-area silicon-strip detector located upstream of a dipole magnet with a bending power of about 4 Tm, and three stations of silicon-strip detectors and straw drift tubes placed downstream. The combined tracking system provides a momentum measurement with relative uncertainty that varies from 0.4% at 5 GeV/ c to 0.6% at 100 GeV/ c , and impact parameter resolution of 20 μm for tracks with large p_T . Different types of charged hadrons are distinguished by information from two ring-imaging Cherenkov detectors. Photon, electron and hadron candidates are identified by a calorimeter system consisting of scintillating-pad and preshower detectors, an electromagnetic calorimeter and a hadronic calorimeter. Muons are identified by a system composed of alternating layers of iron and multiwire proportional chambers.

The trigger consists of a hardware stage, based on information from the calorimeter and muon systems, followed by a software stage, which applies a full event reconstruction. The events used in this analysis are selected at the hardware stage by requiring a cluster in the calorimeters with transverse energy greater than 3.6 GeV. The software trigger requires a two-, three- or four-track secondary vertex (SV) with a large sum of the p_T of the particles and a significant displacement from the primary pp interaction vertices (PVs). At least one charged particle should have $p_T > 1.7$ GeV/ c and χ_{IP}^2 with respect to any PV greater than 16, where χ_{IP}^2 is defined as the difference in fit χ^2 of a given PV reconstructed with and without the considered track. A multivariate algorithm is used for the identification of SVs consistent with the decay of a b hadron.

Simulated collision events are used to estimate the efficiency of the reconstruction and selection steps for signal as well as background b -hadron decay modes. In the simulation, pp collisions are generated using PYTHIA [13] with a specific LHCb configuration [14]. Decays of hadronic particles are described by EVTGEN [15], in which final-state radiation is generated using PHOTOS [16]. The interaction of the generated particles with the detector and its response are implemented using the GEANT4 toolkit [17, 18] as described in ref. [19].

3 Event selection

Since the $\Lambda_b^0 \rightarrow \Lambda_c^+(\rightarrow pK^-\pi^+)\pi^-$ and $\bar{B}^0 \rightarrow D^+(\rightarrow K^-\pi^+\pi^+)\pi^-$ decays have the same topology, the criteria used to select them are chosen to be similar. This minimises the systematic uncertainty on the ratio of the selection efficiencies. Following the trigger selection, a preselection is applied using the reconstructed masses, decay times and vertex qualities of the b -hadron and c -hadron candidates. Further separation between signal and background

is achieved using a boosted decision tree (BDT) [20]. The BDT is trained and tested on a sample of $\bar{B}_s^0 \rightarrow D_s^+ \pi^-$ events from the same data set as the signal events. This sample of events is not used elsewhere in the analysis. For the signal, a weighted data sample based on the *sPlot* technique [21] is used. A training sample representative of combinatorial background is selected from B_s^0 candidates with mass greater than $5445 \text{ MeV}/c^2$. The variables with the most discriminating power are found to be the χ_{IP}^2 of the b -hadron candidate with respect to the PV, the p_{T} of the final-state particles, and the angle between the b -hadron momentum vector and the vector connecting its production and decay vertices. In events with multiple PVs, the b hadron is associated to the PV giving the smallest χ_{IP}^2 .

The BDT requirement is chosen to maximise the signal yield divided by the square root of the sum of the signal and background yields. It rejects approximately 84% of the combinatorial background events while retaining approximately 84% of the signal events. The D^+ (Λ_c^+) candidates are identified by requiring the invariant mass under the $K^- \pi^+ \pi^+$ ($pK^- \pi^+$) hypothesis to fall within the range 1844–1890 (2265–2305) MeV/c^2 . The mass resolution of the charm hadrons is approximately $6 \text{ MeV}/c^2$.

The ratio of selection efficiencies is evaluated using simulated events. The $D^+ \rightarrow K^- \pi^+ \pi^+$ decay is generated using the known Dalitz structure [22], while the $\Lambda_c^+ \rightarrow pK^- \pi^+$ decay is generated using a combination of non-resonant and resonant decay modes with proportions according to ref. [23]. Interference effects in the Λ_c^+ decay are not taken into account. Consistency checks, using a phase-space only model for the $\Lambda_c^+ \rightarrow pK^- \pi^+$ decay, show negligible differences in the relative efficiencies. The distributions of the input variables to the BDT are compared in data and simulation. Good agreement is observed for most variables. The largest deviation is seen for quantities related to the track quality. The simulated events are reweighted so that the distributions of these quantities reproduce the distributions in data.

The final stage of the event selection applies particle identification (PID) criteria on all tracks, based on the differences in the natural logarithm of the likelihood between the pion, kaon and proton hypotheses [24]. The PID performance as a function of the p_{T} and η of the charged particle is estimated from data. This is performed using calibration samples, selected using only kinematic criteria, and consisting of approximately 27 million $D^{*-} \rightarrow \bar{D}^0(K^+ \pi^-) \pi^-$ decays for kaons and pions, and 13 million $\Lambda \rightarrow p \pi^-$ decays for protons. The size of the proton calibration sample is small at high p_{T} of the proton and does not allow a reliable estimate of the efficiency of the proton PID requirement in this kinematic region. Hence, proton PID criteria are only applied to candidates restricted to a kinematic region in proton momentum and pseudorapidity corresponding to low- p_{T} protons. Outside of this region, no PID criteria are imposed on the proton.

The ratio of total selection efficiencies, $\varepsilon_{\bar{B}^0 \rightarrow D^+ \pi^-} / \varepsilon_{\Lambda_b^0 \rightarrow \Lambda_c^+ \pi^-}$, is shown in figure 1. Fluctuations are included in the calculation of the efficiency-corrected yield ratio.

4 Event yields

The dependences of $f_{\Lambda_b^0}/f_d$ on the p_{T} and η of the b hadron are studied in the ranges $1.5 < p_{\text{T}} < 40 \text{ GeV}/c$ and $2 < \eta < 5$. The event sample is sub-divided in 20 bins in p_{T} and 10 bins in η , with bin boundaries chosen to obtain approximately equal numbers

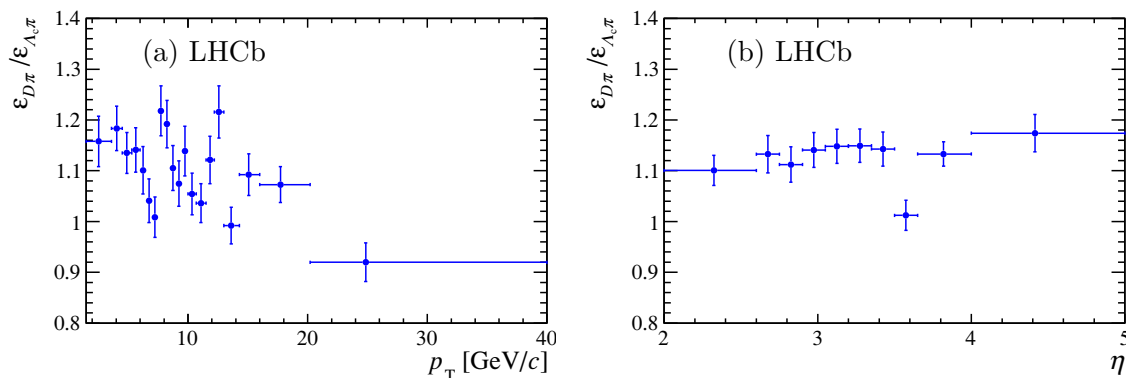


Figure 1. Ratio of total selection efficiencies in bins of the (a) p_T and (b) η of the b hadron. The horizontal error bars indicate the range of each bin in p_T or η respectively.

of $\bar{B}^0 \rightarrow D^+\pi^-$ candidates per bin. The bin centres are obtained from simulated events without any selection applied, and are defined as the mean of the average p_T or η of the $\Lambda_b^0 \rightarrow \Lambda_c^+\pi^-$ and $\bar{B}^0 \rightarrow D^+\pi^-$ samples in each bin.

The yields of the two decay modes are determined from extended maximum likelihood fits to the unbinned mass distributions of the reconstructed b -hadron candidates, in each bin of p_T or η . To improve the mass resolution, the value of the beauty hadron mass is refit with the invariant mass of the charm hadron constrained to its known value [10]. Example fits in the p_T bin with the lowest fitted signal yield and in an arbitrarily chosen η bin are shown in figure 2 for $\Lambda_c^+\pi^-$ and $D^+\pi^-$ candidates. The total signal yields, obtained from fits to the total event samples, are $44\,859 \pm 229$ for the $\Lambda_b^0 \rightarrow \Lambda_c^+\pi^-$ sample and $106\,197 \pm 344$ for the $\bar{B}^0 \rightarrow D^+\pi^-$ sample.

The signal mass shape is described by a modified Gaussian distribution with power-law tails on either side to model the radiative tail and non-Gaussian detector effects. The parameters of the tails are obtained from simulated events and fixed in the fit. The mean and the width of the Gaussian distribution are allowed to vary.

Three classes of background are considered: partially reconstructed decays with or without misidentified tracks, fully reconstructed decays where at least one track is misidentified, and combinatorial background. The shapes of the invariant mass distributions for the partially reconstructed decays are obtained using large samples of simulated events. For the $\bar{B}^0 \rightarrow D^+\pi^-$ sample, the decays $\bar{B}^0 \rightarrow D^+\rho^-$ and $\bar{B}^0 \rightarrow D^{*+}\pi^-$ are modelled with non-parametric distributions [25]. The main sources for the $\Lambda_b^0 \rightarrow \Lambda_c^+\pi^-$ sample are $\Lambda_b^0 \rightarrow \Lambda_c^+\rho^-$ and $\Lambda_b^0 \rightarrow \Sigma_c^+\pi^-$ decays, which are modelled with a bifurcated Gaussian function. All these processes involve a neutral pion that is not included in the candidate’s reconstruction.

The invariant mass distributions of the misidentified decays are affected by the PID criteria. The shapes are obtained from simulated events, reweighted according to the momentum-dependent particle identification efficiency, with the mass hypothesis of the signal applied. The $\bar{B}^0 \rightarrow D^+\pi^-$ background in the $\Lambda_b^0 \rightarrow \Lambda_c^+\pi^-$ sample is most abundant in the highest p_T bins, since the proton PID criteria are least effective in this kinematic region.

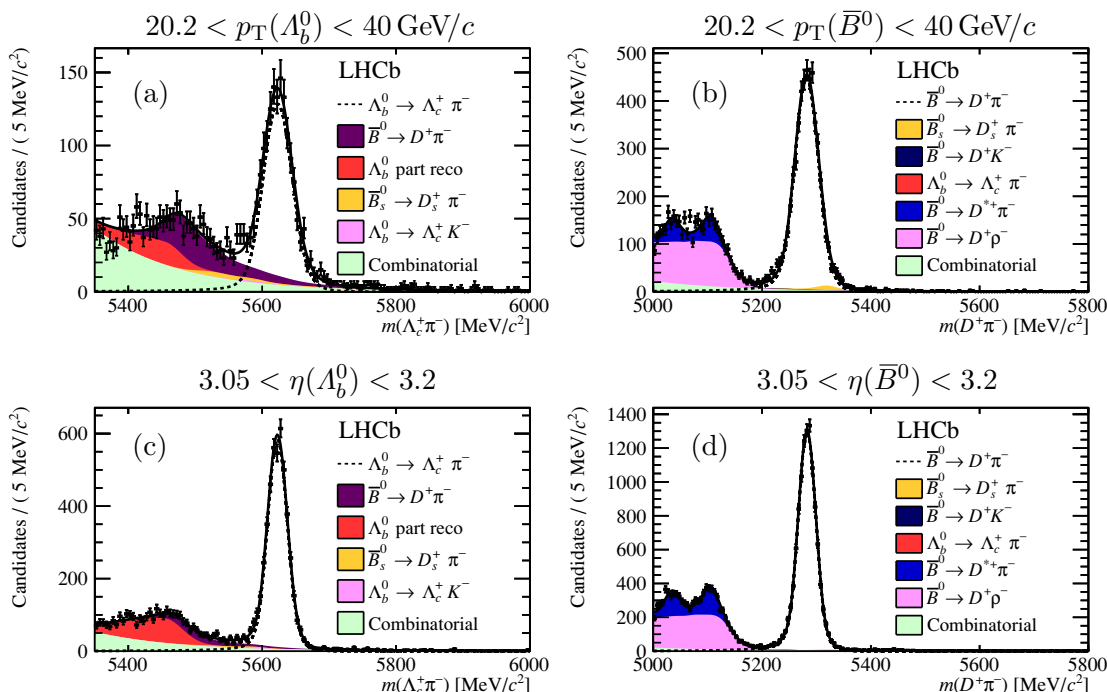


Figure 2. Invariant mass distributions of (a,c) $\Lambda_c^+ \pi^-$ candidates and (b,d) $D^+ \pi^-$ candidates for specific ranges in p_T and η of the b hadron, with fit projections overlaid. The different components are defined in the legend, where “part reco” refers to the sum of partially reconstructed decays.

The Cabibbo-suppressed decays $\Lambda_b^0 \rightarrow \Lambda_c^+ K^-$ and $\bar{B}^0 \rightarrow D^+ K^-$ contribute to the background in the $\Lambda_b^0 \rightarrow \Lambda_c^+ \pi^-$ and $\bar{B}^0 \rightarrow D^+ \pi^-$ fits, respectively, when the kaon of the b -hadron decay is misidentified as a pion. The yields of these backgrounds relative to the signal yield are constrained in the fits, using LHCb measurements of the relevant ratios of branching fractions [9, 26] and the misidentification probabilities with their associated uncertainties.

The combinatorial background consists of events with random pions, kaons and protons forming a mis-reconstructed D^+ or Λ_c^+ candidate, as well as genuine D^+ or Λ_c^+ hadrons, that combine with a random pion. The combinatorial background is modelled with an exponential shape. The slope is fixed in the fit in each kinematic bin to the value found from a fit to the total sample.

5 Results

The study of the dependences of $f_{\Lambda_b^0}/f_d$ on the p_T and η of the b hadron and the measurement of the branching fraction of $\Lambda_b^0 \rightarrow \Lambda_c^+ \pi^-$ decays are performed using candidates restricted to the fiducial region $1.5 < p_T < 40$ GeV/c and $2 < \eta < 5$. A discussion on the systematic uncertainties related to these measurements can be found in the next section.

The ratio of efficiency-corrected event yields as a function of p_T is shown in figure 3(a), and is fitted with an exponential function,

$$\mathcal{R}(p_T) = a + \exp(b + c \times p_T[\text{GeV}/c]), \quad (5.1)$$

with

$$\begin{aligned} a &= +0.181 \pm 0.018 \pm 0.026, \\ b &= -0.391 \pm 0.023 \begin{smallmatrix} +0.069 \\ -0.067 \end{smallmatrix}, \\ c &= -0.095 \pm 0.007 \pm 0.014 [\text{GeV}/c]^{-1}, \end{aligned}$$

where the first uncertainties are statistical and the second systematic. The correlation matrix of the parameters is

$$\rho(a, b, c) = \begin{pmatrix} 1 & -0.22 & -0.94 \\ -0.22 & 1 & -0.10 \\ -0.94 & -0.10 & 1 \end{pmatrix}.$$

The correlation between the parameters leads to a relatively large apparent uncertainty on the individual parameters. Systematic uncertainties are not included in this matrix. The χ^2/ndf value of the fit is 23.3/17, which corresponds to a p-value of 0.14.

The η dependence is described by a linear function,

$$\mathcal{R}(\eta) = a + b \times (\eta - \bar{\eta}), \tag{5.2}$$

with

$$\begin{aligned} a &= 0.464 \pm 0.003 \begin{smallmatrix} +0.008 \\ -0.010 \end{smallmatrix}, \\ b &= 0.081 \pm 0.005 \begin{smallmatrix} +0.013 \\ -0.009 \end{smallmatrix}, \\ \bar{\eta} &= 3.198, \end{aligned}$$

where the first uncertainties are statistical and the second systematic. The offset $\bar{\eta}$ is fixed to the average value of the measured η distribution. The correlation between the two fit parameters is negligible for this choice of $\bar{\eta}$. The χ^2/ndf value of the fit is 13.1/8, corresponding to a p-value of 0.11.

To extract the scale factor \mathcal{S} given in eq. (1.2), the normalisation of $\mathcal{R}(x)$, with fixed parameters a, b and c , is allowed to vary in a fit to the published $f_{\Lambda_b^0}/f_d$ data [7], as shown in figure 3(b). The result quoted in ref. [7] was measured as a function of the p_T of the $\Lambda_c^+ \mu^-$ system. A shift, estimated from simulation, is applied to the p_T values to obtain the corresponding average p_T of the b hadron for each bin. Furthermore, the semileptonic results are updated using recent determinations of $\mathcal{B}(\Lambda_c^+ \rightarrow pK^- \pi^+) = (6.84 \pm 0.24 \begin{smallmatrix} +0.21 \\ -0.27 \end{smallmatrix})\%$ [27] and the ratio of lifetimes $(\tau_{B^+} + \tau_{B^0})/2\tau_{\Lambda_b^0} = 1.071 \pm 0.008$ [28, 29].

The following value of the scale factor \mathcal{S} is determined,

$$\mathcal{S} = 0.834 \pm 0.006 \begin{smallmatrix} \text{hadronic} \\ \text{(stat)} \end{smallmatrix} \begin{smallmatrix} +0.023 \\ -0.021 \end{smallmatrix} \begin{smallmatrix} \text{semileptonic} \\ \text{(syst)} \end{smallmatrix} \pm 0.027 \begin{smallmatrix} \text{semileptonic} \\ \text{(stat)} \end{smallmatrix} \begin{smallmatrix} +0.058 \\ -0.062 \end{smallmatrix} \begin{smallmatrix} \text{semileptonic} \\ \text{(syst)} \end{smallmatrix},$$

where the statistical and systematic uncertainties associated with the hadronic and semileptonic measurement are shown separately. The χ^2/ndf value of the fit is 8.68/3, which corresponds to a p-value of 0.03.

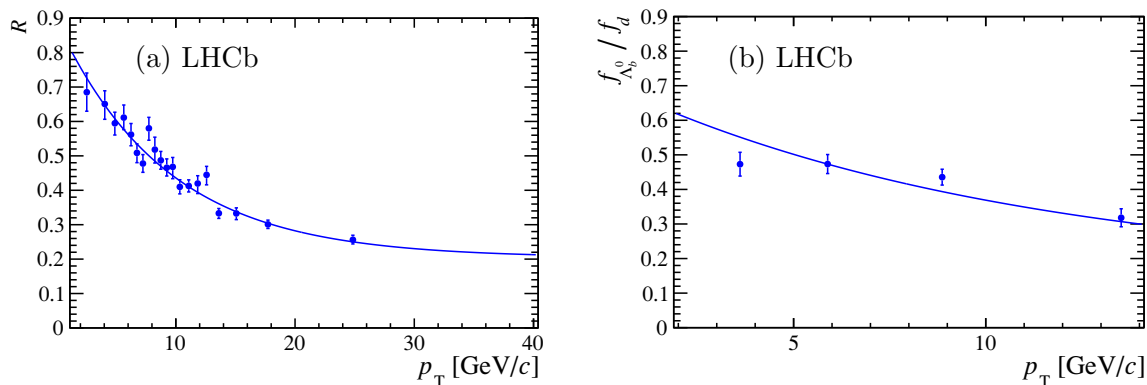


Figure 3. (a) Dependence of the efficiency-corrected ratio of yields, \mathcal{R} , between $\Lambda_b^0 \rightarrow \Lambda_c^+ \pi^-$ and $\bar{B}^0 \rightarrow D^+ \pi^-$ decays on the p_T of the beauty hadron, fitted with an exponential function. The error bars on the data show the statistical and systematic uncertainties added in quadrature. (b) The resulting parametrisation is then fitted to the rescaled $f_{\Lambda_b^0}/f_d$ measurements from the semileptonic analysis [7], to obtain the scale factor \mathcal{S} . The error bars include only the statistical uncertainty.

By multiplying the ratio of the efficiency-corrected yields \mathcal{R} with the scale factor \mathcal{S} , the dependences of $f_{\Lambda_b^0}/f_d$ on p_T and η are obtained. The p_T dependence is described with the exponential function

$$f_{\Lambda_b^0}/f_d(p_T) = a' + \exp(b' + c' \times p_T [\text{GeV}/c]), \quad (5.3)$$

with

$$\begin{aligned} a' &= +0.151 \pm 0.016 \begin{matrix} +0.024 \\ -0.025 \end{matrix}, \\ b' &= -0.573 \pm 0.040 \begin{matrix} +0.101 \\ -0.097 \end{matrix}, \\ c' &= -0.095 \pm 0.007 \pm 0.014 [\text{GeV}/c]^{-1}, \end{aligned}$$

where the first uncertainty is the combined statistical and the second is the combined systematic from the hadronic and semileptonic measurements. The correlations between the three fit parameters change due to the uncertainty on the scale factor \mathcal{S} . The correlation matrix of the parameters is

$$\rho(a', b', c') = \begin{pmatrix} 1 & 0.55 & -0.73 \\ 0.55 & 1 & -0.03 \\ -0.73 & -0.03 & 1 \end{pmatrix}.$$

The η dependence is described by the linear function

$$f_{\Lambda_b^0}/f_d(\eta) = a' + b' \times (\eta - \bar{\eta}), \quad (5.4)$$

with

$$\begin{aligned} a' &= 0.387 \pm 0.013 \begin{matrix} +0.028 \\ -0.030 \end{matrix}, \\ b' &= 0.067 \pm 0.005 \begin{matrix} +0.012 \\ -0.009 \end{matrix}, \end{aligned}$$

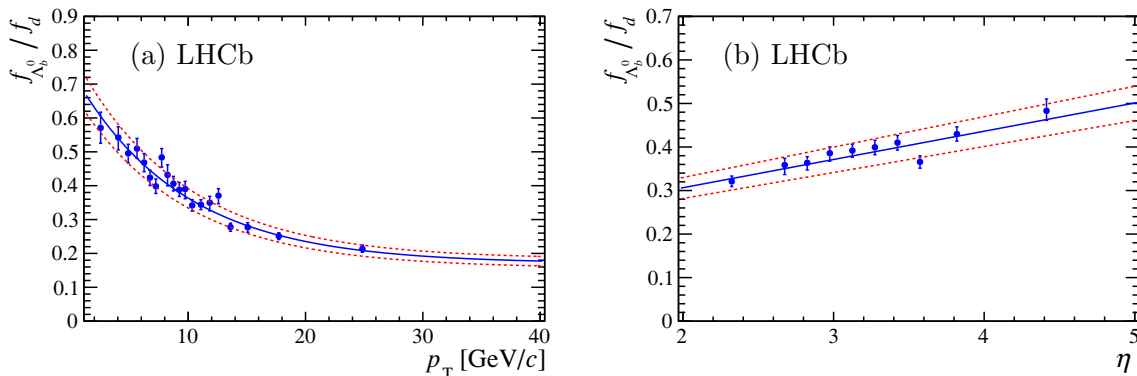


Figure 4. Dependence of $f_{\Lambda_b^0}/f_d$ on the (a) p_T and (b) η of the beauty hadron. To obtain this figure, the ratio of efficiency-corrected event yields is scaled to the absolute value of $f_{\Lambda_b^0}/f_d$ from the semileptonic analysis [7]. The error bars include the statistical and systematic uncertainties associated with the hadronic measurement. The dashed red lines indicate the uncertainty on the scale of $f_{\Lambda_b^0}/f_d$ from the semileptonic analysis.

where the first uncertainty is the combined statistical and the second is the combined systematic from the hadronic and semileptonic measurements. The dependences of $f_{\Lambda_b^0}/f_d$ on the p_T and η of the b hadron are shown in figure 4.

The absolute value for $\mathcal{B}(\Lambda_b^0 \rightarrow \Lambda_c^+ \pi^-)$ is obtained by substituting the results for \mathcal{S} and $\mathcal{B}(\bar{B}^0 \rightarrow D^+ \pi^-) = (2.68 \pm 0.13) \times 10^{-3}$ [10] into eq. (1.2). The value for $\mathcal{B}(\Lambda_c^+ \rightarrow p K^- \pi^+)$ is also used in the determination of $f_{\Lambda_b^0}/f_d$ using semileptonic decays and therefore cancels in the final result. The branching fraction for $\Lambda_b^0 \rightarrow \Lambda_c^+ \pi^-$ is measured to be

$$\mathcal{B}(\Lambda_b^0 \rightarrow \Lambda_c^+ \pi^-) = \left(4.30 \pm 0.03 \begin{smallmatrix} +0.12 \\ -0.11 \end{smallmatrix} \pm 0.26 \pm 0.21 \right) \times 10^{-3},$$

where the first uncertainty is statistical, the second is systematic, the third is from the previous LHCb measurement of $f_{\Lambda_b^0}/f_d$, and the fourth is due to the knowledge of $\mathcal{B}(\bar{B}^0 \rightarrow D^+ \pi^-)$. This value is in agreement with the current world average [10]. It also agrees within 2.4 standard deviations with the recent LHCb measurement using $\Lambda_b^0 \rightarrow \Lambda_c^+(\rightarrow p K_s^0) \pi^-$ decays [30], taking into account the correlated uncertainty from the semileptonic value for $f_{\Lambda_b^0}/f_d$ (6.1%). Combining the two LHCb measurements, and using a consistent value for the lifetime ratio of $(\tau_{B^+} + \tau_{B^0})/2\tau_{\Lambda_b^0} = 1.071 \pm 0.008$, we obtain $\mathcal{B}(\Lambda_b^0 \rightarrow \Lambda_c^+ \pi^-) = (4.46 \pm 0.36) \times 10^{-3}$, where the uncertainty is the combined statistical and systematic uncertainty of both measurements.

6 Systematic uncertainties

Systematic uncertainties on the measurement of the relative efficiency-corrected event yields of the $\Lambda_b^0 \rightarrow \Lambda_c^+ \pi^-$ and $\bar{B}^0 \rightarrow D^+ \pi^-$ decay modes relate to the fit models and to the efficiencies of the PID, BDT and trigger selections. The effect of each systematic uncertainty on the efficiency-corrected yield ratio is calculated separately for each bin of p_T or η . The systematic uncertainties are considered to be correlated across the bins, unless mentioned otherwise. The effect of the systematic uncertainties on the model of the $\mathcal{R}(x)$ dependence

	p_T bins			η bins		$\mathcal{B}(A_b^0 \rightarrow A_c^+ \pi^-)$
	$\mathcal{R} = a + \exp(b + c \times p_T)$			$\mathcal{R} = a + b \times (\eta - \bar{\eta})$		
	a	b	c	a	b	
Fit model						
Signal	+0.7% -0.4%	+0.5% -0.2%	+0.2% -0.3%	+0.3% -0.1%	+1.1% -1.8%	+0.2% -0.1%
Background	+5.5% -1.7%	+2.8% -2.1%	+2.6% -1.1%	+0.6% -0.1%	+2.4% -4.7%	+0.6% -0.0%
Efficiencies						
PID	0.0%	0.5%	2.5%	-1.3%	12.7%	-1.1%
BDT	+5.8% -7.6%	-15.1% +14.2%	+9.6% -10.2%	+1.3% -1.3%	+4.7% -4.8%	+2.3% -2.2%
Sample size	$\pm 12.1\%$	$\pm 9.0\%$	$\pm 10.8\%$	$\pm 0.9\%$	$\pm 9.3\%$	$\pm 1.2\%$
Trigger	0.9%	1.0%	1.0%	-0.3%	-0.1%	-0.3%
Other						
Bin centre	$\pm 0.3\%$	$\pm 0.3\%$	$\pm 0.1\%$	$\pm 0.1\%$	$\pm 1.3\%$	0.0%
Total	+14.6% -14.5%	+17.1% -17.7%	+14.9% -14.9%	+1.8% -2.1%	+16.6% -11.6%	+2.6% -2.8%

Table 1. Relative systematic uncertainties for the measurements of $\mathcal{R}(x)$ (first five columns) and $\mathcal{B}(A_b^0 \rightarrow A_c^+ \pi^-)$ (last column). The uncertainties from the various sources are uncorrelated and added in quadrature to obtain the total uncertainty. Sample size refers to the size of the simulated events sample.

and the measurement of $\mathcal{B}(A_b^0 \rightarrow A_c^+ \pi^-)$ are determined by refitting the data points when the \mathcal{R} value in each bin is varied by its associated uncertainty. The various sources of systematic uncertainty are discussed below and summarised in table 1.

The uncertainty due to the modelling of the signal shape is estimated by replacing the modified Gaussian with two modified Gaussians, which share the same mean but are allowed to have different widths. In addition, the parameters that describe the tails are varied by $\pm 10\%$ relative to their nominal values, which is the maximum variation found for these parameters when leaving them free in the fit. This affects the ratio of yields by a maximum of 0.3%.

A possible variation of the slope of the combinatorial background shape across the bins is observed in a data sample of $A_c^+ \pi^+$ candidates. To account for this, the slope is varied from $\pm 50\%$ in the lowest p_T or η bin to $\mp 50\%$ in the highest p_T or η bin. The signal yield ratio varies by less than 1%, with the exception of one p_T bin which shows a variation of approximately 2%.

The uncertainty on the shapes of partially reconstructed backgrounds is estimated by modelling them with a non-parametric distribution [25] for $A_b^0 \rightarrow \Sigma_c^+ \pi^-$ and $A_b^0 \rightarrow A_c^+ \rho^-$ decays and with two modified Gaussian distributions with tails on either side for the $\bar{B}^0 \rightarrow D^{*+} \pi^-$ shape. The effect on the signal yield ratio is below 0.5% in most bins, increasing to about 2% for the highest p_T bin.

The contribution of b -hadron decays without an intermediate c hadron is ignored in the fit. To evaluate the systematic uncertainty due to these decays, the b -hadron mass

spectra for candidates in the sidebands of the c -hadron mass distribution are examined. A contribution of 0.4% relative to the signal yield is found in the $\bar{B}^0 \rightarrow D^+\pi^-$ decay mode, and its full size is taken as systematic uncertainty. No contribution is seen in the $\Lambda_b^0 \rightarrow \Lambda_c^+\pi^-$ decay mode and no systematic uncertainty is assigned.

The uncertainty on the PID efficiency and misidentification rate is estimated by comparing the PID performance measured using simulated D^* and Λ calibration samples with that observed in simulated signal events. The efficiency ratio varies by between 1% and 4% across the bins.

As discussed in section 3, the simulated events are reweighted so that the distributions of quantities related to the track quality match the distributions observed in data. The systematic uncertainty on the selection efficiency is obtained by recalculating the efficiency without this reweighting. The yield ratio varies by between 0.2% and 6%. In addition, there is a 5% statistical uncertainty per bin due to the simulated sample size, which is uncorrelated across bins.

The uncertainty due to the trigger efficiency, caused by possible differences in the response to a proton compared to a charged pion in the calorimeter, is estimated to be about 0.4%, taking into account that at most 10% of the events containing $\Lambda_b^0 \rightarrow \Lambda_c^+\pi^-$ candidates are triggered by the proton. The systematic uncertainty due to the choice of bin centre is evaluated by redefining the bin centres using the average p_T or η of the Λ_b^0 or B^0 sample only, instead of the mean of the Λ_b^0 and B^0 samples.

7 Conclusions

The dependences of the production rate of Λ_b^0 baryons with respect to B^0 mesons are measured as functions of the transverse momentum p_T and of the pseudorapidity η of the b hadron. The p_T dependence is accurately described by an exponential function. The ratio of fragmentation fractions $f_{\Lambda_b^0}/f_d$ decreases by a factor of three in the range $1.5 < p_T < 40$ GeV/ c . The ratio of fragmentation fractions $f_{\Lambda_b^0}/f_d$ versus η is described by a linear dependence in the range $2 < \eta < 5$.

The absolute scale of $f_{\Lambda_b^0}/f_d$ is fixed using the measurement of $f_{\Lambda_b^0}/f_d$ from semileptonic b -hadron decays [7]. The branching fraction of the decay $\Lambda_b^0 \rightarrow \Lambda_c^+\pi^-$ is determined with a total precision of 8%,

$$\mathcal{B}(\Lambda_b^0 \rightarrow \Lambda_c^+\pi^-) = \left(4.30 \pm 0.03 \begin{smallmatrix} +0.12 \\ -0.11 \end{smallmatrix} \pm 0.26 \pm 0.21\right) \times 10^{-3},$$

which is the most precise determination of a branching fraction of a beauty baryon to date.

Acknowledgments

We express our gratitude to our colleagues in the CERN accelerator departments for the excellent performance of the LHC. We thank the technical and administrative staff at the LHCb institutes. We acknowledge support from CERN and from the national agencies: CAPES, CNPq, FAPERJ and FINEP (Brazil); NSFC (China); CNRS/IN2P3 and Region Auvergne (France); BMBF, DFG, HGF and MPG (Germany); SFI (Ireland);

INFN (Italy); FOM and NWO (The Netherlands); SCSR (Poland); MEN/IFA (Romania); MinES, Rosatom, RFBR and NRC “Kurchatov Institute” (Russia); MinECo, XuntaGal and GENCAT (Spain); SNSF and SER (Switzerland); NASU (Ukraine); STFC and the Royal Society (United Kingdom); NSF (U.S.A.). We also acknowledge the support received from EPLANET, Marie Curie Actions and the ERC under FP7. The Tier1 computing centres are supported by IN2P3 (France), KIT and BMBF (Germany), INFN (Italy), NWO and SURF (The Netherlands), PIC (Spain), GridPP (United Kingdom). We are indebted to the communities behind the multiple open source software packages on which we depend. We are also thankful for the computing resources and the access to software R&D tools provided by Yandex LLC (Russia).

Open Access. This article is distributed under the terms of the Creative Commons Attribution License ([CC-BY 4.0](https://creativecommons.org/licenses/by/4.0/)), which permits any use, distribution and reproduction in any medium, provided the original author(s) and source are credited.

References

- [1] A.V. Berezhnoy and A.K. Likhoded, *The relative yields of heavy hadrons as function of transverse momentum at LHC experiments*, [arXiv:1309.1979](https://arxiv.org/abs/1309.1979) [[INSPIRE](#)].
- [2] I. Dunietz, *CP violation with beautiful baryons*, *Z. Phys.* **C 56** (1992) 129 [[INSPIRE](#)].
- [3] LHCb collaboration, *Measurement of the Ξ_b^- and Ω_b^- baryon lifetimes*, *Phys. Lett.* **B 736** (2014) 154 [[arXiv:1405.1543](https://arxiv.org/abs/1405.1543)] [[INSPIRE](#)].
- [4] HEAVY FLAVOR AVERAGING GROUP collaboration, Y. Amhis et al., *Averages of B-Hadron, C-Hadron and tau-lepton properties as of early 2012*, [arXiv:1207.1158](https://arxiv.org/abs/1207.1158) [[INSPIRE](#)].
- [5] CDF collaboration, T. Aaltonen et al., *Measurement of Ratios of Fragmentation Fractions for Bottom Hadrons in $p\bar{p}$ Collisions at $\sqrt{s} = 1.96$ TeV*, *Phys. Rev.* **D 77** (2008) 072003 [[arXiv:0801.4375](https://arxiv.org/abs/0801.4375)] [[INSPIRE](#)].
- [6] CDF collaboration, T. Aaltonen et al., *First Measurement of the Ratio of Branching Fractions $B(\Lambda_b^0 \rightarrow \Lambda_c^+ \mu^- \bar{\nu}_\mu)/B(\Lambda_b^0 \rightarrow \Lambda_c^+ \pi^-)$* , *Phys. Rev.* **D 79** (2009) 032001 [[arXiv:0810.3213](https://arxiv.org/abs/0810.3213)] [[INSPIRE](#)].
- [7] LHCb collaboration, *Measurement of b-hadron production fractions in 7 TeVpp collisions*, *Phys. Rev.* **D 85** (2012) 032008 [[arXiv:1111.2357](https://arxiv.org/abs/1111.2357)] [[INSPIRE](#)].
- [8] CMS collaboration, *Measurement of the Λ_b cross section and the $\bar{\Lambda}_b$ to Λ_b ratio with $J/\Psi\Lambda$ decays in pp collisions at $\sqrt{s} = 7$ TeV*, *Phys. Lett.* **B 714** (2012) 136 [[arXiv:1205.0594](https://arxiv.org/abs/1205.0594)] [[INSPIRE](#)].
- [9] LHCb collaboration, *Measurement of the fragmentation fraction ratio f_s/f_d and its dependence on B meson kinematics*, *JHEP* **04** (2013) 001 [[arXiv:1301.5286](https://arxiv.org/abs/1301.5286)] [[INSPIRE](#)].
- [10] PARTICLE DATA GROUP collaboration, J. Beringer et al., *Review of Particle Physics (RPP)*, *Phys. Rev.* **D 86** (2012) 010001 [[INSPIRE](#)].
- [11] CLEO collaboration, S. Dobbs et al., *Measurement of absolute hadronic branching fractions of D mesons and $e^+e^- \rightarrow D\bar{D}$ cross-sections at the $\Psi(3770)$* , *Phys. Rev.* **D 76** (2007) 112001 [[arXiv:0709.3783](https://arxiv.org/abs/0709.3783)] [[INSPIRE](#)].
- [12] LHCb collaboration, *The LHCb Detector at the LHC*, 2008 *JINST* **3** S08005 [[INSPIRE](#)].

- [13] T. Sjöstrand, S. Mrenna and P.Z. Skands, *PYTHIA 6.4 Physics and Manual*, *JHEP* **05** (2006) 026 [[hep-ph/0603175](#)] [[INSPIRE](#)].
- [14] I. Belyaev et al., *Handling of the generation of primary events in GAUSS, the LHCb simulation framework*, *IEEE Nucl. Sci. Symp. Conf. Rec.* (2010) 1155.
- [15] D.J. Lange, *The EvtGen particle decay simulation package*, *Nucl. Instrum. Meth. A* **462** (2001) 152 [[INSPIRE](#)].
- [16] P. Golonka and Z. Was, *PHOTOS Monte Carlo: A precision tool for QED corrections in Z and W decays*, *Eur. Phys. J. C* **45** (2006) 97 [[hep-ph/0506026](#)] [[INSPIRE](#)].
- [17] GEANT4 collaboration, J. Allison et al., *Geant4 developments and applications*, *IEEE Trans. Nucl. Sci.* **53** (2006) 270.
- [18] GEANT4 collaboration, S. Agostinelli et al., *GEANT4: A simulation toolkit*, *Nucl. Instrum. Meth. A* **506** (2003) 250 [[INSPIRE](#)].
- [19] M. Clemencic et al., *The LHCb simulation application, Gauss: Design, evolution and experience*, *J. Phys. Conf. Ser.* **331** (2011) 032023 [[INSPIRE](#)].
- [20] L. Breiman, J.H. Friedman, R.A. Olshen and C.J. Stone, *Classification and regression trees*, Wadsworth international group, Belmont, California, U.S.A. (1984).
- [21] M. Pivk and F.R. Le Diberder, *SPlot: A statistical tool to unfold data distributions*, *Nucl. Instrum. Meth. A* **555** (2005) 356 [[physics/0402083](#)] [[INSPIRE](#)].
- [22] CLEO collaboration, G. Bonvicini et al., *Dalitz plot analysis of the $D^+ \rightarrow K^- \pi^+ \pi^+$ decay*, *Phys. Rev. D* **78** (2008) 052001 [[arXiv:0802.4214](#)] [[INSPIRE](#)].
- [23] E791 collaboration, E.M. Aitala et al., *Multidimensional resonance analysis of $\Lambda_c^+ \rightarrow pK^- \pi^+$* , *Phys. Lett. B* **471** (2000) 449 [[hep-ex/9912003](#)] [[INSPIRE](#)].
- [24] LHCb RICH GROUP collaboration, *Performance of the LHCb RICH detector at the LHC*, *Eur. Phys. J. C* **73** (2013) 2431 [[arXiv:1211.6759](#)] [[INSPIRE](#)].
- [25] K.S. Cranmer, *Kernel estimation in high-energy physics*, *Comput. Phys. Commun.* **136** (2001) 198 [[hep-ex/0011057](#)] [[INSPIRE](#)].
- [26] LHCb collaboration, *Studies of beauty baryon decays to $D^0 p h^-$ and $\Lambda_c^+ h^-$ final states*, *Phys. Rev. D* **89** (2014) 032001 [[arXiv:1311.4823](#)] [[INSPIRE](#)].
- [27] BELLE collaboration, A. Zupanc et al., *Measurement of the Branching Fraction $Br(\Lambda_c^+ \rightarrow pK^- \pi^+)$* , *Phys. Rev. Lett.* **113** (2014) 042002 [[arXiv:1312.7826](#)] [[INSPIRE](#)].
- [28] LHCb collaboration, *Measurements of the B^+ , B^0 , B_s^0 meson and Λ_b^0 baryon lifetimes*, *JHEP* **04** (2014) 114 [[arXiv:1402.2554](#)] [[INSPIRE](#)].
- [29] LHCb collaboration, *Precision measurement of the ratio of the Λ_b^0 to \bar{B}^0 lifetimes*, *Phys. Lett. B* **734** (2014) 122 [[arXiv:1402.6242](#)] [[INSPIRE](#)].
- [30] LHCb collaboration, *Searches for Λ_b^0 and Ξ_b^0 decays to $K_S^0 p \pi^-$ and $K_S^0 p K^-$ final states with first observation of the $\Lambda_b^0 \rightarrow K_S^0 p \pi^-$ decay*, *JHEP* **04** (2014) 087 [[arXiv:1402.0770](#)] [[INSPIRE](#)].

The LHCb collaboration

R. Aaij⁴¹, B. Adeva³⁷, M. Adinolfi⁴⁶, A. Affolder⁵², Z. Ajaltouni⁵, J. Albrecht⁹, F. Alessio³⁸, M. Alexander⁵¹, S. Ali⁴¹, G. Alkhazov³⁰, P. Alvarez Cartelle³⁷, A.A. Alves Jr^{25,38}, S. Amato², S. Amerio²², Y. Amhis⁷, L. An³, L. Anderlini^{17,g}, J. Anderson⁴⁰, R. Andreassen⁵⁷, M. Andreotti^{16,f}, J.E. Andrews⁵⁸, R.B. Appleby⁵⁴, O. Aquines Gutierrez¹⁰, F. Archilli³⁸, A. Artamonov³⁵, M. Artuso⁵⁹, E. Aslanides⁶, G. Auriemma^{25,n}, M. Baalouch⁵, S. Bachmann¹¹, J.J. Back⁴⁸, A. Badalov³⁶, V. Balagura³¹, W. Baldini¹⁶, R.J. Barlow⁵⁴, C. Barschel³⁸, S. Barsuk⁷, W. Barter⁴⁷, V. Batozskaya²⁸, Th. Bauer⁴¹, A. Bay³⁹, J. Beddow⁵¹, F. Bedeschi²³, I. Bediaga¹, S. Belogurov³¹, K. Belous³⁵, I. Belyaev³¹, E. Ben-Haim⁸, G. Bencivenni¹⁸, S. Benson⁵⁰, J. Benton⁴⁶, A. Berezhnoy³², R. Bernet⁴⁰, M.-O. Bettler⁴⁷, M. van Beuzekom⁴¹, A. Bien¹¹, S. Bifani⁴⁵, T. Bird⁵⁴, A. Bizzeti^{17,i}, P.M. Bjørnstad⁵⁴, T. Blake⁴⁸, F. Blanc³⁹, J. Blouw¹⁰, S. Blusk⁵⁹, V. Bocci²⁵, A. Bondar³⁴, N. Bondar^{30,38}, W. Bonivento^{15,38}, S. Borghi⁵⁴, A. Borgia⁵⁹, M. Borsato⁷, T.J.V. Bowcock⁵², E. Bowen⁴⁰, C. Bozzi¹⁶, T. Brambach⁹, J. van den Brand⁴², J. Bressieux³⁹, D. Brett⁵⁴, M. Britsch¹⁰, T. Britton⁵⁹, N.H. Brook⁴⁶, H. Brown⁵², A. Bursche⁴⁰, G. Busetto^{22,q}, J. Buytaert³⁸, S. Cadeddu¹⁵, R. Calabrese^{16,f}, O. Callot⁷, M. Calvi^{20,k}, M. Calvo Gomez^{36,o}, A. Camboni³⁶, P. Campana^{18,38}, D. Campora Perez³⁸, A. Carbone^{14,d}, G. Carboni^{24,l}, R. Cardinale^{19,38,j}, A. Cardini¹⁵, H. Carranza-Mejia⁵⁰, L. Carson⁵⁰, K. Carvalho Akiba², G. Casse⁵², L. Cassina²⁰, L. Castillo Garcia³⁸, M. Cattaneo³⁸, Ch. Cauet⁹, R. Cenci⁵⁸, M. Charles⁸, Ph. Charpentier³⁸, S.-F. Cheung⁵⁵, N. Chiapolini⁴⁰, M. Chrzasteczko^{40,26}, K. Ciba³⁸, X. Cid Vidal³⁸, G. Ciezarek⁵³, P.E.L. Clarke⁵⁰, M. Clemencic³⁸, H.V. Cliff⁴⁷, J. Closier³⁸, C. Coca²⁹, V. Coco³⁸, J. Cogan⁶, E. Cogneras⁵, P. Collins³⁸, A. Comerma-Montells³⁶, A. Contu^{15,38}, A. Cook⁴⁶, M. Coombes⁴⁶, S. Coquereau⁸, G. Corti³⁸, M. Corvo^{16,f}, I. Counts⁵⁶, B. Couturier³⁸, G.A. Cowan⁵⁰, D.C. Craik⁴⁸, M. Cruz Torres⁶⁰, S. Cunliffe⁵³, R. Currie⁵⁰, C. D'Ambrosio³⁸, J. Dalseno⁴⁶, P. David⁸, P.N.Y. David⁴¹, A. Davis⁵⁷, K. De Bruyn⁴¹, S. De Capua⁵⁴, M. De Cian¹¹, J.M. De Miranda¹, L. De Paula², W. De Silva⁵⁷, P. De Simone¹⁸, D. Decamp⁴, M. Deckenhoff⁹, L. Del Buono⁸, N. Déleage⁴, D. Derkach⁵⁵, O. Deschamps⁵, F. Dettori⁴², A. Di Canto³⁸, H. Dijkstra³⁸, S. Donleavy⁵², F. Dordei¹¹, M. Dorigo³⁹, A. Dosil Suárez³⁷, D. Dossett⁴⁸, A. Dovbnya⁴³, F. Dupertuis³⁹, P. Durante³⁸, R. Dzhelyadin³⁵, A. Dziurda²⁶, A. Dzyuba³⁰, S. Easo⁴⁹, U. Egede⁵³, V. Egorychev³¹, S. Eidelman³⁴, S. Eisenhardt⁵⁰, U. Eitschberger⁹, R. Ekelhof⁹, L. Eklund^{51,38}, I. El Rifai⁵, Ch. Elsasser⁴⁰, S. Esen¹¹, T. Evans⁵⁵, A. Falabella^{16,f}, C. Färber¹¹, C. Farinelli⁴¹, S. Farry⁵², D. Ferguson⁵⁰, V. Fernandez Albor³⁷, F. Ferreira Rodrigues¹, M. Ferro-Luzzi³⁸, S. Filippov³³, M. Fiore^{16,f}, M. Fiorini^{16,f}, M. Firlej²⁷, C. Fitzpatrick³⁸, T. Fiutowski²⁷, M. Fontana¹⁰, F. Fontanelli^{19,j}, R. Forty³⁸, O. Francisco², M. Frank³⁸, C. Frei³⁸, M. Frosini^{17,38,g}, J. Fu²¹, E. Furfaro^{24,l}, A. Gallas Torreira³⁷, D. Galli^{14,d}, S. Gambetta^{19,j}, M. Gandelman², P. Gandini⁵⁹, Y. Gao³, J. Garofoli⁵⁹, J. Garra Tico⁴⁷, L. Garrido³⁶, C. Gaspar³⁸, R. Gauld⁵⁵, L. Gavardi⁹, E. Gersabeck¹¹, M. Gersabeck⁵⁴, T. Gershon⁴⁸, Ph. Ghez⁴, A. Gianelle²², S. Giani³⁹, V. Gibson⁴⁷, L. Giubega²⁹, V.V. Gligorov³⁸, C. Göbel⁶⁰, D. Golubkov³¹, A. Golutvin^{53,31,38}, A. Gomes^{1,a}, H. Gordon³⁸, C. Gotti²⁰, M. Grabalosa Gándara⁵, R. Graciani Diaz³⁶, L.A. Granado Cardoso³⁸, E. Graugés³⁶, G. Graziani¹⁷, A. Greco²⁹, E. Greening⁵⁵, S. Gregson⁴⁷, P. Griffith⁴⁵, L. Grillo¹¹, O. Grünberg⁶², B. Gui⁵⁹, E. Gushchin³³, Yu. Guz^{35,38}, T. Gys³⁸, C. Hadjivasiliou⁵⁹, G. Haefeli³⁹, C. Haen³⁸, S.C. Haines⁴⁷, S. Hall⁵³, B. Hamilton⁵⁸, T. Hampson⁴⁶, X. Han¹¹, S. Hansmann-Menzemer¹¹, N. Harnew⁵⁵, S.T. Harnew⁴⁶, J. Harrison⁵⁴, T. Hartmann⁶², J. He³⁸, T. Head³⁸, V. Heijne⁴¹, K. Hennessy⁵², P. Henrard⁵, L. Henry⁸, J.A. Hernando Morata³⁷, E. van Herwijnen³⁸, M. Heß⁶², A. Hicheur¹, D. Hill⁵⁵, M. Hoballah⁵, C. Hombach⁵⁴, W. Hulsbergen⁴¹, P. Hunt⁵⁵, N. Hussain⁵⁵, D. Hutchcroft⁵², D. Hynds⁵¹, M. Idzik²⁷, P. Ilten⁵⁶, R. Jacobsson³⁸, A. Jaeger¹¹, J. Jalocha⁵⁵, E. Jans⁴¹, P. Jaton³⁹,

A. Jawahery⁵⁸, M. Jezabek²⁶, F. Jing³, M. John⁵⁵, D. Johnson⁵⁵, C.R. Jones⁴⁷, C. Joram³⁸,
 B. Jost³⁸, N. Jurik⁵⁹, M. Kaballo⁹, S. Kandybei⁴³, W. Kanso⁶, M. Karacson³⁸, T.M. Karbach³⁸,
 M. Kelsey⁵⁹, I.R. Kenyon⁴⁵, T. Ketel⁴², B. Khanji²⁰, C. Khurewathanakul³⁹, S. Klaver⁵⁴,
 O. Kochebina⁷, M. Kolpin¹¹, I. Komarov³⁹, R.F. Koopman⁴², P. Koppenburg^{41,38}, M. Korolev³²,
 A. Kozlinskiy⁴¹, L. Kravchuk³³, K. Kreplin¹¹, M. Kreps⁴⁸, G. Krocker¹¹, P. Krokovny³⁴,
 F. Kruse⁹, M. Kucharczyk^{20,26,38,k}, V. Kudryavtsev³⁴, K. Kurek²⁸, T. Kvaratskheliya³¹,
 V.N. La Thi³⁹, D. Lacarrere³⁸, G. Lafferty⁵⁴, A. Lai¹⁵, D. Lambert⁵⁰, R.W. Lambert⁴²,
 E. Lanciotti³⁸, G. Lanfranchi¹⁸, C. Langenbruch³⁸, B. Langhans³⁸, T. Latham⁴⁸, C. Lazzeroni⁴⁵,
 R. Le Gac⁶, J. van Leerdam⁴¹, J.-P. Lees⁴, R. Lefèvre⁵, A. Leflat³², J. Lefrançois⁷, S. Leo²³,
 O. Leroy⁶, T. Lesiak²⁶, B. Leverington¹¹, Y. Li³, M. Liles⁵², R. Lindner³⁸, C. Linn³⁸,
 F. Lionetto⁴⁰, B. Liu¹⁵, G. Liu³⁸, S. Lohn³⁸, I. Longstaff⁵¹, J.H. Lopes², N. Lopez-March³⁹,
 P. Lowdon⁴⁰, H. Lu³, D. Lucchesi^{22,q}, H. Luo⁵⁰, A. Lupato²², E. Luppi^{16,f}, O. Lupton⁵⁵,
 F. Machefert⁷, I.V. Machikhiliyan³¹, F. Maciuc²⁹, O. Maev³⁰, S. Malde⁵⁵, G. Manca^{15,e},
 G. Mancinelli⁶, M. Manzali^{16,f}, J. Maratas⁵, J.F. Marchand⁴, U. Marconi¹⁴, C. Marin Benito³⁶,
 P. Marino^{23,s}, R. Märki³⁹, J. Marks¹¹, G. Martellotti²⁵, A. Martens⁸, A. Martín Sánchez⁷,
 M. Martinelli⁴¹, D. Martinez Santos⁴², F. Martinez Vidal⁶⁴, D. Martins Tostes², A. Massafferri¹,
 R. Matev³⁸, Z. Mathe³⁸, C. Matteuzzi²⁰, A. Mazurov^{16,38,f}, M. McCann⁵³, J. McCarthy⁴⁵,
 A. McNab⁵⁴, R. McNulty¹², B. McKelley⁵², B. Meadows^{57,55}, F. Meier⁹, M. Meissner¹¹,
 M. Merk⁴¹, D.A. Milanese⁸, M.-N. Minard⁴, J. Molina Rodriguez⁶⁰, S. Monteil⁵, D. Moran⁵⁴,
 M. Morandin²², P. Morawski²⁶, A. Mordà⁶, M.J. Morello^{23,s}, J. Moron²⁷, R. Mountain⁵⁹,
 F. Muheim⁵⁰, K. Müller⁴⁰, R. Muresan²⁹, B. Muster³⁹, P. Naik⁴⁶, T. Nakada³⁹, R. Nandakumar⁴⁹,
 I. Nasteva¹, M. Needham⁵⁰, N. Neri²¹, S. Neubert³⁸, N. Neufeld³⁸, M. Neuner¹¹, A.D. Nguyen³⁹,
 T.D. Nguyen³⁹, C. Nguyen-Mau^{39,p}, M. Nicol⁷, V. Niess⁵, R. Niet⁹, N. Nikitin³², T. Nikodem¹¹,
 A. Novoselov³⁵, A. Oblakowska-Mucha²⁷, V. Obraztsov³⁵, S. Oggero⁴¹, S. Ogilvy⁵¹,
 O. Okhrimenko⁴⁴, R. Oldeman^{15,e}, G. Onderwater⁶⁵, M. Orlandea²⁹, J.M. Otalora Goicochea²,
 P. Owen⁵³, A. Oyanguren⁶⁴, B.K. Pal⁵⁹, A. Palano^{13,c}, F. Palombo^{21,t}, M. Palutan¹⁸,
 J. Panman³⁸, A. Papanestis^{49,38}, M. Pappagallo⁵¹, C. Parkes⁵⁴, C.J. Parkinson⁹, G. Passaleva¹⁷,
 G.D. Patel⁵², M. Patel⁵³, C. Patrignani^{19,j}, A. Pazos Alvarez³⁷, A. Pearce⁵⁴, A. Pellegrino⁴¹,
 M. Pepe Altarelli³⁸, S. Perazzini^{14,d}, E. Perez Trigo³⁷, P. Perret⁵, M. Perrin-Terrin⁶,
 L. Pescatore⁴⁵, E. Pesen⁶⁶, K. Petridis⁵³, A. Petrolini^{19,j}, E. Picatoste Olloqui³⁶, B. Pietrzyk⁴,
 T. Pilar⁴⁸, D. Pinci²⁵, A. Pistone¹⁹, S. Playfer⁵⁰, M. Plo Casasus³⁷, F. Polci⁸, A. Poluektov^{48,34},
 E. Polcarpo², A. Popov³⁵, D. Popov¹⁰, B. Popovici²⁹, C. Potterat², A. Powell⁵⁵,
 J. Prisciandaro³⁹, A. Pritchard⁵², C. Prouve⁴⁶, V. Pugatch⁴⁴, A. Puig Navarro³⁹, G. Punzi^{23,r},
 W. Qian⁴, B. Rachwal²⁶, J.H. Rademacker⁴⁶, B. Rakotomiarmanana³⁹, M. Rama¹⁸,
 M.S. Rangel², I. Raniuk⁴³, N. Rauschmayr³⁸, G. Raven⁴², S. Reichert⁵⁴, M.M. Reid⁴⁸,
 A.C. dos Reis¹, S. Ricciardi⁴⁹, A. Richards⁵³, K. Rinnert⁵², V. Rives Molina³⁶,
 D.A. Roa Romero⁵, P. Robbe⁷, A.B. Rodrigues¹, E. Rodrigues⁵⁴, P. Rodriguez Perez⁵⁴,
 S. Roiser³⁸, V. Romanovsky³⁵, A. Romero Vidal³⁷, M. Rotondo²², J. Rouvinet³⁹, T. Ruf³⁸,
 F. Ruffini²³, H. Ruiz³⁶, P. Ruiz Valls⁶⁴, G. Sabatino^{25,l}, J.J. Saborido Silva³⁷, N. Sagidova³⁰,
 P. Sail⁵¹, B. Saitta^{15,e}, V. Salustino Guimaraes², C. Sanchez Mayordomo⁶⁴, B. Sanmartin Sedes³⁷,
 R. Santacesaria²⁵, C. Santamarina Rios³⁷, E. Santovetti^{24,l}, M. Sapunov⁶, A. Sarti^{18,m},
 C. Satriano^{25,n}, A. Satta²⁴, M. Savrie^{16,f}, D. Savrina^{31,32}, M. Schiller⁴², H. Schindler³⁸,
 M. Schlupp⁹, M. Schmelling¹⁰, B. Schmidt³⁸, O. Schneider³⁹, A. Schopper³⁸, M.-H. Schune⁷,
 R. Schwemmer³⁸, B. Sciascia¹⁸, A. Sciubba²⁵, M. Seco³⁷, A. Semennikov³¹, K. Senderowska²⁷,
 I. Sepp⁵³, N. Serra⁴⁰, J. Serrano⁶, L. Sestini²², P. Seyfert¹¹, M. Shapkin³⁵, I. Shapoval^{16,43,f},
 Y. Shcheglov³⁰, T. Shears⁵², L. Shekhtman³⁴, V. Shevchenko⁶³, A. Shires⁹, R. Silva Coutinho⁴⁸,
 G. Simi²², M. Sirendi⁴⁷, N. Skidmore⁴⁶, T. Skwarnicki⁵⁹, N.A. Smith⁵², E. Smith^{55,49}, E. Smith⁵³,
 J. Smith⁴⁷, M. Smith⁵⁴, H. Snoek⁴¹, M.D. Sokoloff⁵⁷, F.J.P. Soler⁵¹, F. Soomro³⁹, D. Souza⁴⁶,

B. Souza De Paula², B. Spaan⁹, A. Sparkes⁵⁰, F. Spinella²³, P. Spradlin⁵¹, F. Stagni³⁸, S. Stahl¹¹, O. Steinkamp⁴⁰, O. Stenyakin³⁵, S. Stevenson⁵⁵, S. Stoica²⁹, S. Stone⁵⁹, B. Storaci⁴⁰, S. Stracka^{23,38}, M. Straticiu²⁹, U. Straumann⁴⁰, R. Stroili²², V.K. Subbiah³⁸, L. Sun⁵⁷, W. Sutcliffe⁵³, K. Swientek²⁷, S. Swientek⁹, V. Syropoulos⁴², M. Szczekowski²⁸, P. Szczypka^{39,38}, D. Szilard², T. Szumlak²⁷, S. T'Jampens⁴, M. Teklishyn⁷, G. Tellarini^{16,f}, E. Teodorescu²⁹, F. Teubert³⁸, C. Thomas⁵⁵, E. Thomas³⁸, J. van Tilburg⁴¹, V. Tisserand⁴, M. Tobin³⁹, S. Tolck⁴², L. Tomassetti^{16,f}, D. Tonelli³⁸, S. Topp-Joergensen⁵⁵, N. Torr⁵⁵, E. Tournefier⁴, S. Tourneur³⁹, M.T. Tran³⁹, M. Tresch⁴⁰, A. Tsaregorodtsev⁶, P. Tsopelas⁴¹, N. Tuning⁴¹, M. Ubeda Garcia³⁸, A. Ukleja²⁸, A. Ustyuzhanin⁶³, U. Uwer¹¹, V. Vagnoni¹⁴, G. Valenti¹⁴, A. Vallier⁷, R. Vazquez Gomez¹⁸, P. Vazquez Regueiro³⁷, C. Vázquez Sierra³⁷, S. Vecchi¹⁶, J.J. Velthuis⁴⁶, M. Veltri^{17,h}, G. Veneziano³⁹, M. Vesterinen¹¹, B. Viaud⁷, D. Vieira², M. Vieites Diaz³⁷, X. Vilasis-Cardona^{36,o}, A. Vollhardt⁴⁰, D. Volyanskyy¹⁰, D. Voong⁴⁶, A. Vorobyev³⁰, V. Vorobyev³⁴, C. Voß⁶², H. Voss¹⁰, J.A. de Vries⁴¹, R. Waldi⁶², C. Wallace⁴⁸, R. Wallace¹², J. Walsh²³, S. Wandernoth¹¹, J. Wang⁵⁹, D.R. Ward⁴⁷, N.K. Watson⁴⁵, A.D. Webber⁵⁴, D. Websdale⁵³, M. Whitehead⁴⁸, J. Wicht³⁸, D. Wiedner¹¹, G. Wilkinson⁵⁵, M.P. Williams⁴⁵, M. Williams⁵⁶, F.F. Wilson⁴⁹, J. Wimberley⁵⁸, J. Wishahi⁹, W. Wislicki²⁸, M. Witek²⁶, G. Wormser⁷, S.A. Wotton⁴⁷, S. Wright⁴⁷, S. Wu³, K. Wyllie³⁸, Y. Xie⁶¹, Z. Xing⁵⁹, Z. Xu³⁹, Z. Yang³, X. Yuan³, O. Yushchenko³⁵, M. Zangoli¹⁴, M. Zavertyaev^{10,b}, F. Zhang³, L. Zhang⁵⁹, W.C. Zhang¹², Y. Zhang³, A. Zhelezov¹¹, A. Zhokhov³¹, L. Zhong³, A. Zvyagin³⁸.

¹ *Centro Brasileiro de Pesquisas Físicas (CBPF), Rio de Janeiro, Brazil*

² *Universidade Federal do Rio de Janeiro (UFRJ), Rio de Janeiro, Brazil*

³ *Center for High Energy Physics, Tsinghua University, Beijing, China*

⁴ *LAPP, Université de Savoie, CNRS/IN2P3, Annecy-Le-Vieux, France*

⁵ *Clermont Université, Université Blaise Pascal, CNRS/IN2P3, LPC, Clermont-Ferrand, France*

⁶ *CPPM, Aix-Marseille Université, CNRS/IN2P3, Marseille, France*

⁷ *LAL, Université Paris-Sud, CNRS/IN2P3, Orsay, France*

⁸ *LPNHE, Université Pierre et Marie Curie, Université Paris Diderot, CNRS/IN2P3, Paris, France*

⁹ *Fakultät Physik, Technische Universität Dortmund, Dortmund, Germany*

¹⁰ *Max-Planck-Institut für Kernphysik (MPIK), Heidelberg, Germany*

¹¹ *Physikalisches Institut, Ruprecht-Karls-Universität Heidelberg, Heidelberg, Germany*

¹² *School of Physics, University College Dublin, Dublin, Ireland*

¹³ *Sezione INFN di Bari, Bari, Italy*

¹⁴ *Sezione INFN di Bologna, Bologna, Italy*

¹⁵ *Sezione INFN di Cagliari, Cagliari, Italy*

¹⁶ *Sezione INFN di Ferrara, Ferrara, Italy*

¹⁷ *Sezione INFN di Firenze, Firenze, Italy*

¹⁸ *Laboratori Nazionali dell'INFN di Frascati, Frascati, Italy*

¹⁹ *Sezione INFN di Genova, Genova, Italy*

²⁰ *Sezione INFN di Milano Bicocca, Milano, Italy*

²¹ *Sezione INFN di Milano, Milano, Italy*

²² *Sezione INFN di Padova, Padova, Italy*

²³ *Sezione INFN di Pisa, Pisa, Italy*

²⁴ *Sezione INFN di Roma Tor Vergata, Roma, Italy*

²⁵ *Sezione INFN di Roma La Sapienza, Roma, Italy*

²⁶ *Henryk Niewodniczanski Institute of Nuclear Physics Polish Academy of Sciences, Kraków, Poland*

²⁷ *AGH - University of Science and Technology, Faculty of Physics and Applied Computer Science, Kraków, Poland*

²⁸ *National Center for Nuclear Research (NCBJ), Warsaw, Poland*

²⁹ *Horia Hulubei National Institute of Physics and Nuclear Engineering, Bucharest-Magurele, Romania*

- ³⁰ Petersburg Nuclear Physics Institute (PNPI), Gatchina, Russia
- ³¹ Institute of Theoretical and Experimental Physics (ITEP), Moscow, Russia
- ³² Institute of Nuclear Physics, Moscow State University (SINP MSU), Moscow, Russia
- ³³ Institute for Nuclear Research of the Russian Academy of Sciences (INR RAN), Moscow, Russia
- ³⁴ Budker Institute of Nuclear Physics (SB RAS) and Novosibirsk State University, Novosibirsk, Russia
- ³⁵ Institute for High Energy Physics (IHEP), Protvino, Russia
- ³⁶ Universitat de Barcelona, Barcelona, Spain
- ³⁷ Universidad de Santiago de Compostela, Santiago de Compostela, Spain
- ³⁸ European Organization for Nuclear Research (CERN), Geneva, Switzerland
- ³⁹ Ecole Polytechnique Fédérale de Lausanne (EPFL), Lausanne, Switzerland
- ⁴⁰ Physik-Institut, Universität Zürich, Zürich, Switzerland
- ⁴¹ Nikhef National Institute for Subatomic Physics, Amsterdam, The Netherlands
- ⁴² Nikhef National Institute for Subatomic Physics and VU University Amsterdam, Amsterdam, The Netherlands
- ⁴³ NSC Kharkiv Institute of Physics and Technology (NSC KIPT), Kharkiv, Ukraine
- ⁴⁴ Institute for Nuclear Research of the National Academy of Sciences (KINR), Kyiv, Ukraine
- ⁴⁵ University of Birmingham, Birmingham, United Kingdom
- ⁴⁶ H.H. Wills Physics Laboratory, University of Bristol, Bristol, United Kingdom
- ⁴⁷ Cavendish Laboratory, University of Cambridge, Cambridge, United Kingdom
- ⁴⁸ Department of Physics, University of Warwick, Coventry, United Kingdom
- ⁴⁹ STFC Rutherford Appleton Laboratory, Didcot, United Kingdom
- ⁵⁰ School of Physics and Astronomy, University of Edinburgh, Edinburgh, United Kingdom
- ⁵¹ School of Physics and Astronomy, University of Glasgow, Glasgow, United Kingdom
- ⁵² Oliver Lodge Laboratory, University of Liverpool, Liverpool, United Kingdom
- ⁵³ Imperial College London, London, United Kingdom
- ⁵⁴ School of Physics and Astronomy, University of Manchester, Manchester, United Kingdom
- ⁵⁵ Department of Physics, University of Oxford, Oxford, United Kingdom
- ⁵⁶ Massachusetts Institute of Technology, Cambridge, MA, United States
- ⁵⁷ University of Cincinnati, Cincinnati, OH, United States
- ⁵⁸ University of Maryland, College Park, MD, United States
- ⁵⁹ Syracuse University, Syracuse, NY, United States
- ⁶⁰ Pontifícia Universidade Católica do Rio de Janeiro (PUC-Rio), Rio de Janeiro, Brazil, associated to ²
- ⁶¹ Institute of Particle Physics, Central China Normal University, Wuhan, Hubei, China, associated to ³
- ⁶² Institut für Physik, Universität Rostock, Rostock, Germany, associated to ¹¹
- ⁶³ National Research Centre Kurchatov Institute, Moscow, Russia, associated to ³¹
- ⁶⁴ Instituto de Fisica Corpuscular (IFIC), Universitat de Valencia-CSIC, Valencia, Spain, associated to ³⁶
- ⁶⁵ KVI - University of Groningen, Groningen, The Netherlands, associated to ⁴¹
- ⁶⁶ Celal Bayar University, Manisa, Turkey, associated to ³⁸
- ^a Universidade Federal do Triângulo Mineiro (UFTM), Uberaba-MG, Brazil
- ^b P.N. Lebedev Physical Institute, Russian Academy of Science (LPI RAS), Moscow, Russia
- ^c Università di Bari, Bari, Italy
- ^d Università di Bologna, Bologna, Italy
- ^e Università di Cagliari, Cagliari, Italy
- ^f Università di Ferrara, Ferrara, Italy
- ^g Università di Firenze, Firenze, Italy
- ^h Università di Urbino, Urbino, Italy
- ⁱ Università di Modena e Reggio Emilia, Modena, Italy

- ^j *Università di Genova, Genova, Italy*
- ^k *Università di Milano Bicocca, Milano, Italy*
- ^l *Università di Roma Tor Vergata, Roma, Italy*
- ^m *Università di Roma La Sapienza, Roma, Italy*
- ⁿ *Università della Basilicata, Potenza, Italy*
- ^o *LIFAELS, La Salle, Universitat Ramon Llull, Barcelona, Spain*
- ^p *Hanoi University of Science, Hanoi, Viet Nam*
- ^q *Università di Padova, Padova, Italy*
- ^r *Università di Pisa, Pisa, Italy*
- ^s *Scuola Normale Superiore, Pisa, Italy*
- ^t *Università degli Studi di Milano, Milano, Italy*